Rangeland Condition Monitoring Asssement and Projection (RCMAP) 1985-2021 Factsheet

1. Description:
   In collaboration with the Bureau of Land Management (BLM), the U.S. Geological Survey (USGS) has produced annual maps of fractional component cover for 1985-2021 (37 years). Components mapped: annual herbaceous, perennial herbaceous, total herbaceous, sagebrush, non-sagebrush shrub, total shrub, litter, bare ground, and tree canopy cover.
2. Intended Use:
   Annual fractional cover maps can assist land managers and scientists to monitor changes to vegetation composition, evaluate past management practices, target future improvements, determine locations of critical wildlife habitat, assess impacts of climate change and interannual variation, and appraise landscape health and fragmentation
3. Training data are obtained from various sources (Table 1, Figure 1).

**Table 1. Training data for RCMAP fractional component time-series.**

| Source | *n* | Notes | Spatial Extent | Temporal Extent |
|---|---|---|---|---|
| RCMAP High-Resolution Sites Degraded to 30-m | 56,426,952 | Data for each high-resolution site is predicted from 60-120 ocular observations, collected at the 2-m imagery resolution (see Rigge et al. 2020) | 331, ~15 x ~15km sites | 2006-2017 |
| RCMAP Landsat-Scale Plots | 8,691 | Field observations located between high-resolution sites | Average of 2, 30-m transects or ocular estimation | 2013-2021 |
| BLM Analysis Inventory and Monitoring (AIM) | 28,971 | Bureau of Land Management (BLM AIM, 2021) | Average of 3, 50-m transects | 2011-2021 |
| BLM Landscape Monitoring Framework (LMF) | 16,674 | Bureau of Land Management | Average of 3, 50-m transects | 2004-2019 |
| LANDFIRE Public Database | 183,861 | Curated from several sources: USFS Vegetation and Fuel Plot Data, USGS National Gap Analysis Program (GAP), NPS Inventory and Monitoring (I&M), State Inventory Data (see LANDFIRE, 2022) | Various methods | 1985-2015 |
| Total | 56,665,149 | | | 1985-2021 |

**Figure 1. RCMAP training data distrubution**

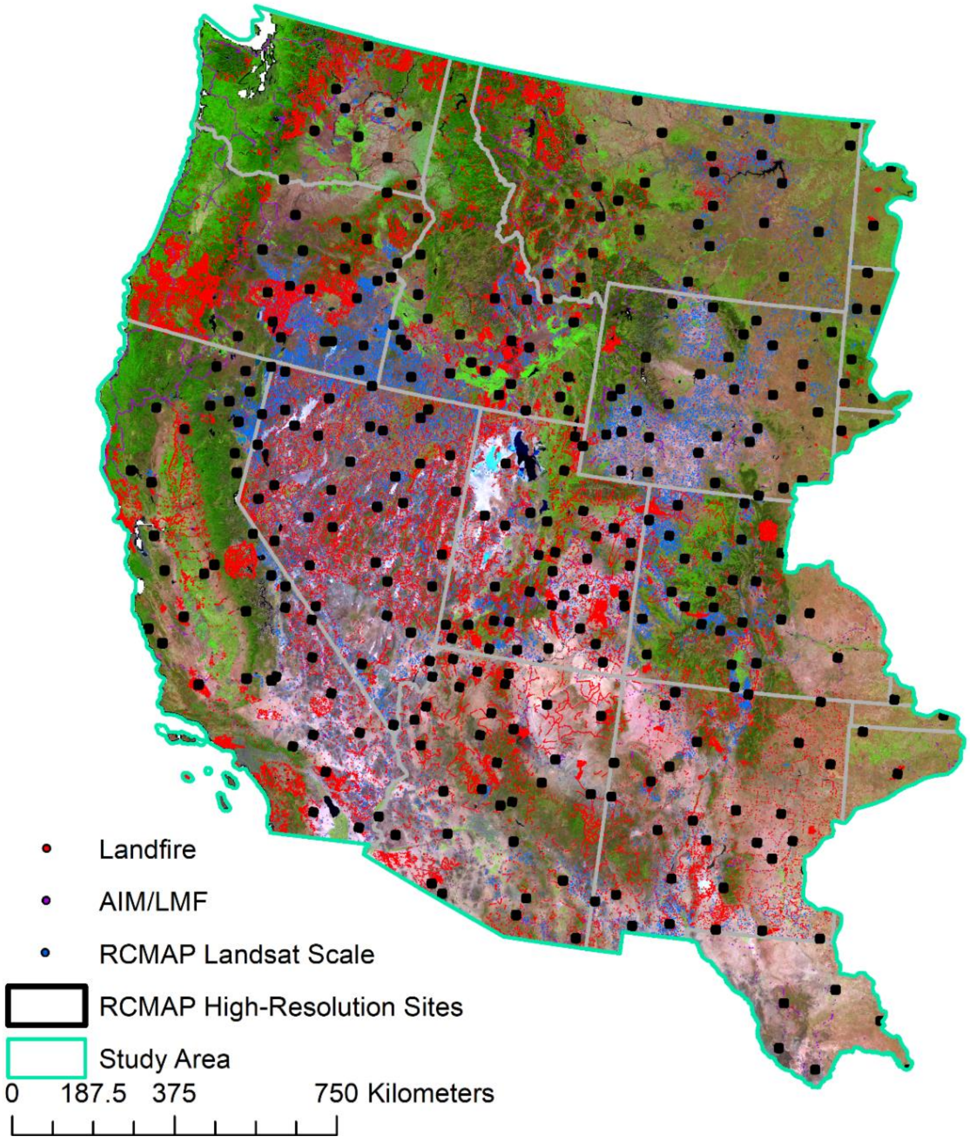


4. Independent Data:
   A) Topographic: slope, aspect, position index, elevation
   B) Landsat Imagery: two median pixel composites for each year: leaf-on, to represent peak vegetation growth and leaf-off, senesced (i.e., brown) conditions (see Table 2 for dates) by mapping region (Figure 2). The composites are further cleaned by identifying pixels with less than 3 clear observations, which tend to be phenologically inconsistent and/or have cloud/shadow/snow contamination and by considering the relevant synthetic dates (see C) in the median value calculation of these locations.
   C) CCDC-Synthetic Imagery: Five months of Continuous Change Detection and Classification (CCDC) synthetic images per year, predicted using models fit to the historical observations for each pixel (see, Zhu et al. 2015). Synthetic images are targeted to preferentially capture the early growing season (see Table 2 for dates).
   D) Landsat Imagery Indices: Normalized Difference Water Index (NDWI), Built-up index (BDI),

Soil Adjusted Vegetation Index (SAVI), tassel cap indices: greenness, wetness, and brightness for leaf-on and leaf-off median composites for each year.

**Table 2. Imagery composite dates by mapping region.**

| Region | Median Composites | | Monthly Synthetic | |
|---|---|---|---|---|
| | Leaf-on | Leaf-off | Leaf-on | Leaf-off |
| Mediterranean California | Dec. 1 – May 30 | Jun. 1 – Oct. 1 | Jan., Feb, | Jun., Sep. |
| Great Basin and Columbia Plateau | Mar. 15 – Jun. | Jul. 1 – Nov. 01 | Mar. - Jun. | Sep. |
| Northern Rocky Mountains | June 15 – Aug. 25 | Apr. 15 – May 15, Sep. 1 – Oct. 15 | Jun.- Aug | Sep., Oct. |
| Northern Great Plains | Apr. 1 – Jun. 30 | Jul. 15 – Nov. 1 | Apr. - Jul. | Sep. |
| Mojave, Sonoran, and Chihuahuan Deserts | Jul. 20 – Oct. 15 | Mar. 1 – Jul. 1 | Aug., Sep. | Mar., Apr., Jun., |
| Southern Mountains | Jun. 1 – Aug. 15 | Apr. 1 – May 1, Sep. 1 – Nov. 1 | Jun. - Aug. | Sep., Oct. |
| Colorado Plateau and Southwest Tablelands | Jun. 1 – Aug. 30 | Sep. 15 – Dec. 1 | Jun. - Aug. | Sep., Nov. |
| Pacific Northwest | May 1- Jul. 20 | Sep. 15 – Dec. 1 | Mar. - Jul. | Oct. |

**Figure 2. RCMAP mapping regions**


5. Model and Post-Processing

   We used neural network models optimized with Keras Tuner that are four layers deep, 128 neurons wide, and with a 20% dropout rate between each layer. For each mapping region, we developed a single neural network model to predict all components. We compared our regression neural network with the results from previous versions of RCMAP that used Cubist: finding all else equal, error rates were reduced by 5-7%.

   We want our products to represent a combination of empirical data and logic-based rules. Therefore, post-processing models are utilized to limit noise and accurately capture post-fire component cover values. Post-processing has been improved with updated fire recovery equations stratified by ecosystem resistance and resilience (R and R) classes (Maestas and Campbell 2016).

6. Validation results

Maps are rigorously validated using field data not included as training (i.e., independent) with data from long-term monitoring sites, and by assessing model fit to training data. Our independent data consists of 1) 1,880 points, each specifically designed to represent a single Landsat pixel, collected from 2013-2020, and 2) long-term monitoring data in southwest Wyoming at 126 plots observed 12 times between 2008 and 2021. The spatial-temporal correlation ($n$ = 1,137) across all 126 plots showed robust correlations for all components, with an $R^2$ of 0.62 for bare ground (RMSE = 11.7%) and 0.47 for shrub cover (RMSE = 8.0%) and average $R^2$ of 0.42 and RMSE of 8.93 across components.

Next, we compared RCMAP data to independent validation sites ($n$ = 1,880) collected from 2013-2020 (Table 3). Correlations between RCMAP and independent validation sites were again robust across all components, with an $R^2$ of 0.75 for bare ground (RMSE = 13.5%) and 0.40 for shrub cover (RMSE = 10.3%) and average $R^2$ of 0.53 and RMSE of 10.4 across components.

Pooling all independent data (long-term monitoring plus independent sites, total $n$ = 3,017): Bare Ground - $R^2$ 0.74, RMSE 12.9, Herbaceous - $R^2$ 0.66, RMSE 11.5, Litter - $R^2$ 0.38, RMSE 8.5, Shrub - $R^2$ 0.40, RMSE 9.6, Sagebrush - $R^2$ 0.38, RMSE 7.2, Annual Herbaceous - $R^2$ 0.56, RMSE 10.1.

**Table 3. Summary of validation results at independent and BLM AIM/LMF sites.**

| Data | Metric | Annual Herb. | Bare Ground | Herb. | Litter | Sagebrush | Shrub | Tree |
|---|---|---|---|---|---|---|---|---|
| Independent | $R^2$ | 0.56 | 0.75 | 0.70 | 0.37 | 0.41 | 0.40 | n/a |
| AIM/LMF | $R^2$ | 0.30 | 0.60 | 0.56 | 0.03 | 0.42 | 0.35 | 0.66 |
| Independent | RMSE | 10.1 | 13.5 | 12.4 | 8.6 | 7.3 | 10.3 | n/a |
| AIM/LMF | RMSE | 15.1 | 24.4 | 21.7 | 12.0 | 8.5 | 11.0 | 7.4 |

We compared RCMAP data to BLM AIM and LMF data ($n$ = 45,132) collected between 2004 and 2021. Correlations between RCMAP and AIM/LMF data were again robust across all components, with an $R^2$ of 0.60 for bare ground, $R^2$ of 0.66 for tree, and 0.35 for shrub cover and average $R^2$ of 0.38 and RMSE of 14.3 across components.

Finally, we conducted a cross-validation of predictions against training data at high-resolution training sites using a random sample of 100,000 points. Cross-validation correlations included an $R^2$ of 0.89 for bare ground (RMSE = 9.7%) and 0.66 for shrub cover (RMSE = 8.3%) and average $R^2$ of 0.76 and RMSE of 7.3 across components. Bare Ground - $R^2$ 0.89, RMSE 9.7, Herbaceous - $R^2$ 0.82, RMSE 7.9, Litter - $R^2$ 0.70, RMSE 5.5, Shrub - $R^2$ 0.66, RMSE 8.3, Sagebrush - $R^2$ 0.66, RMSE 4.1, Annual Herbaceous - $R^2$ 0.75, RMSE 5.4, Tree - $R^2$ 0.83, RMSE 9.7.

Changes observed in both the field and RCMAP data were typically gradual, within-state, changes which are most difficult to resolve, which were often successfully captured. It is important to consider that all accuracy assessments described above are designed to evaluate single-pixel level correspondence. Due to fine-scale landscape heterogeneity this is the most rigorous approach, and most applications looking at broader spatial scales would tend to lower error relative to this analysis.

7. Caveats

CCDC-synthetic data rely on harmonic models to fit the temporal profile of all available clear Landsat data. The algorithm can predict Landsat surface reflectance for any dates. The quality of the model is dependent on the number of clear observations, with increased likelihood of simple models near the end of the time-series (Zhu et al. 2015). Discrete change events are detected as breaks in the temporal profile if their RMSE is more than two times RMSE for six consecutive observations, which creates the potential for a temporal lag for the phenomena to manifest on the synthetic imagery. We do not consider synthetic images to be exact proxies of additional “real” Landsat observations, rather include the data to represent the inter- and intra-annual phenological patterns, which are strongly related to component cover.

The nature of our modeling approach tends to result in bias to underestimating change between periods rather than overestimating change. Most training data was derived from high resolution predictions (Table 1) of component cover which dramatically increases the number and spatial extent of training data. However as these are modeled products, they do contain error (Table 4). Assessments of component predictions at the high-resolution scale demonstrate average accuracy (*r*) by component ranging from 0.90 to 0.97 and absolute error of 1.81 to 4.65%. Error also exists in the other sources of training: BLM AIM, etc.

**Table 4. Test accuracy of high-resolution (2-m) scale predictions of component cover**

| Component | Absolute Error | *r* |
|---|---|---|
| Bare Ground | 4.65 | 0.97 |
| Herbaceous | 4.26 | 0.94 |
| Litter | 3.13 | 0.91 |
| Shrub | 4.55 | 0.94 |
| Sagebrush | 2.66 | 0.90 |
| Annual Herbaceous | 1.81 | 0.94 |

RCMAP products are designed to reflect the ground conditions under the peak of the growing season (i.e., greenest conditions). However, due to image availability and timing of training observations, this may not always be the case. Users are encouraged to evaluate differences between the largest possible units acceptable to their analysis (e.g., compare the population of pixels between two pastures instead of between two pixels) to minimize the impact of error.

8. Related Publications

BLM AIM (2021) Bureau of land management: assessment, inventory, and monitoring. http://aim.landscapetoolbox.org/.

LANDFIRE: Public LANDFIRE Reference Database. (2022, March - last update). U.S. Department of Interior, Geological Survey, and U.S. Department of Agriculture. [Online]. Available: https://landfire.gov/lfrdb_data.php [Accessed 12-3-2021].

Maestas, J., S. Campbell, C. Chambers, M. Pellant, and F. Miller. 2016. Tapping soil survey information for rapid assessment of sagebrush ecosystem resilience and resistance. *Rangelands* 38: 120-128.

Rigge, M., B. Bunde, D. Meyer, H. Shi, and K. Postma. 2021. Rangeland Condition Monitoring Assessment and Projection (RCMAP) Fractional Component Time-Series Across the Western U.S. 1985-2020. U.S. Geological Survey data release, https://doi.org/10.5066/P95IQ4BT.

Rigge, M., C. Homer, L. Cleeves, D. Meyer, B. Bunde, H. Shi, G. Xian, and M. Bobo. 2020. Quantifying western U.S. rangelands as fractional components with multi-resolution remote sensing and in situ data. *Remote Sensing* 12: 412.

Rigge, M., C. Homer, H. Shi, D. Meyer, B. Bunde, B. Granneman, K. Postma, P. Danielson, A. Case, and G. Xian. 2021. Rangeland Fractional Components Across the Western United States from 1985-2018. *Remote Sensing* 13: 813.

Shi, H., M. Rigge, K. Postma, and B. Bunde. 2022. Trends analysis of rangeland condition monitoring assessment and projection (RCMAP) fractional component time series (1985-2020). *GIScience & Remote Sensing* 59: 1243-1265.

Zhu, Z., C. Woodcock, C. Holden, and Z. Yang. 2015. Generating synthetic Landsat images based on all available Landsat data: Predicting Landsat surface reflectance at any given time. *Remote Sensing of Environment* 162, 67–83.